Published in *Proceedings of the 114th International Symposium on Linear Drivers for Industry Applications (LDIA)*, Hannover, Germany, 28-30 june 2023, which should be cited to refer to this work.DOI: 10.1109/LDIA59564.2023.10297536

Design and Simulation of the Electrodynamic Suspension of an Hyperloop Test Vehicle

Maude Fumeaux
Institute of Systems Engineering
School of Engineering, HES-SO
Valais-Wallis
Sion, Switzerland

Maxence Cailleteau
Institute of Mechanical Design,
Materials Science and Packaging
Technologies
School of Engineering, HEIG-VD
Yverdon, Switzerland

David Melly
Institute of Systems Engineering
School of Engineering, HES-SO
Valais-Wallis
Sion, Switzerland

Samuel Chevailler
Institute of Systems Engineering
School of Engineering, HES-SO
Valais-Wallis
Sion, Switzerland
samuel.chevailler@hevs.ch

Joël Cugnoni
Institute of Mechanical Design,
Materials Science and Packaging
Technologies
School of Engineering, HEIG-VD
Yverdon, Switzerland
joel.cugnoni@heig-vd.ch

***Abstract*—This paper deals with the electromagnetic design of a small vehicle designed to be tested in a dedicated vacuum tube. As imposed by the facilities in the tube, the guidance must be passive. Its design is therefore highly dependent on the vehicle dynamic behaviour to ensure that it remains within the limits of its guidance zone. The guidance and levitation are provided by an electrodynamic suspension (EDS) done with a Halbach array interacting with a conductive track. This article mainly focuses on its design and its influence on the dynamic behaviour of the vehicle.**

Keywords—EDS, Vacuum Transportation, FEA, Halbach Array.

I. INTRODUCTION

Vacuum transportation technologies offer several advantages such as low carbon emission and flexibility [1]. To develop and test various technologies relating to this mode of transport, the EuroTube Foundation is developing two vacuum tunnels. The main features of these testing infrastructures are summarized in the following section.

The developed vehicle will allow testing several technologies principle as the passive guidance and levitation systems, different brake systems (mechanic or magnetic), dynamic behaviour along the track, propulsion system, measurement technologies. The paper focuses on the design methodology of the guidance and levitation system and its influence on the dynamic behaviour of the vehicle.

II. SPECIFICATIONS AND VEHICLE CONCEPT

While the focus of this paper is the levitation system and the modelling of the dynamic behaviour of the vehicle, the propulsion launcher as well as the braking system are briefly introduced in the following section.

A. Tube

The vehicle will be first tested in the shortest tube (DemoTube, 120m, internal diameter of 2.2m, built in 2024) under partial vacuum to a pressure down to 1 mbar. Later on, it is planned to test it in the Alphatube (3km, built in 2026).

B. Vehicle

The vehicle (Fig. 1) also includes a battery module, a thermal storage module and an aerodynamic fairing as well as all the interfaces to mount propulsion and levitation modules including sensor for force monitoring. Other sensors are planned to monitor speed/position, pressure, temperature and airgaps.

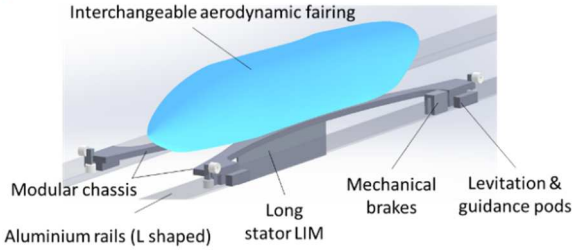

Fig. 1. Developed vehicle

The main specifications of the vehicle are the followings:

- Chassis dimensions 3 m x 1.2 m
- Total mass 134 kg
- Mechanical brake and viscoelastic suspension
- Secondary of the linear motor 1 m x 0.25 m
- Electrodynamic suspension with Halbach array

C. Levitation and guidance

The tube provides electrically conductive rails along the track. Two configurations for the guidance/levitation system, presented in Fig. 2, will be thoroughly analysed. The first configuration is to use two aluminium L-shape rails. The strong side Halbach array is used to levitate and the leakage flux on the side is used for the guidance. The second configuration uses two inclined aluminium plates. The inclination angle α (see Fig. 4) is adapted to vary the ratio levitation force vs. guidance force.

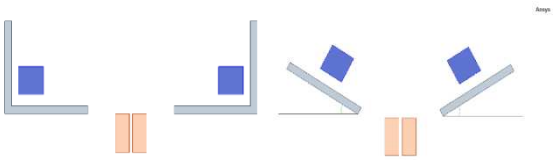

Fig. 2. Studied levitation and guidance configurations

D. Launcher and LIM's secondary

The tube is equipped with a launcher to propel the vehicle. The propulsion is realised with a double-sided induction

motor (DSLIM). The design of the secondary part is let to the user of the tube. Hence, secondary made of aluminium, copper as well as a hybrid secondary iron/alu have been investigated using FEA. The hybrid version was left aside due to high lateral forces in case of airgap eccentricities. The main advantage of the copper plate is to reduce the secondary losses due to a better conductivity. As the short time of the launch is not thermally critical for the secondary and to reduce the mass and the cost of the prototype, the aluminium secondary has been chosen. To limit the influence of transverse edge effect on secondary resistance, the effect of overhangs has been investigated in a 3D FEA model. The length of the overhangs has been chosen equal to 0.8 times the pole pitch. This value is a good compromise between the thrust performance and the volume of the secondary part. To reduce the torque ripple different secondary geometries have also been studied as proposed in [2].

E. Braking System

Additionally, to the mechanical brakes present on the vehicle, concepts for an emergency brake at the end of the track has been studied. The use of the secondary part of the DSLIM has part of an eddy current brake has been investigated. The specifications are to break the vehicle from 18 m/s to standstill over a distance shorter than 3m. An analytical model [3] has been compared to FEA simulation for a double-sided magnet array as presented on the figure below. Each side of the brake consists of 40 poles of 180x60x15mm.

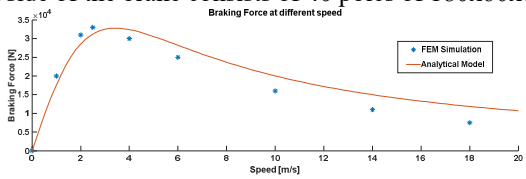

Fig. 3. Braking force for different speeds

III. LEVITATION AND GUIDANCE SYSTEM

A. Approach

In addition to the results and methodology of the design of Halbach arrays for the two rail configurations, the optimal number of magnets constituting the array as well as the electromagnetic damping obtained with a damping aluminium cage is discussed.

B. Influence of rail shape (L versus V at different angle)

This demonstrator will be tested at low speed (v_{max} = 35 m/s), the mechanical properties of the rail and its geometry therefore influence the forces. The right choice of aluminium alloy (resistivity) can slightly improve performances. The thickness of the rail up to 13 mm can significantly improve the levitation of the system depending on the speed. If the Halbach array is used to lift and guide the vehicle, the forces are distributed differently depending on the rail geometry. The studied rail shapes are illustrated in Fig. 4. The L-shaped rails use the side flux leakage of the Halbach array to produce a lateral force to guide the vehicle. In the case of the V-shaped rails, the guidance force depends on the inclination of the rail. Increasing the angle α improves the guidance force but reduces the levitation force. It has been shown that an angle of 10° reproduces similar performances to L-shaped rail in terms of guidance, lift and drag.

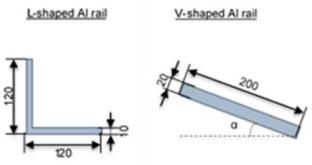

Fig. 4. Rail design

C. Magnet size and number

For the design of this prototype, the quality, the size, the number and the magnetization of PMs are the only modifiable parameters to improve the flight. The chosen magnets are NdFeB45, they allow a good compromise between performances and price. Three different Halbach assemblies are compared and illustrated below.

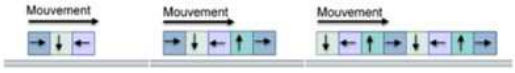

Fig. 5. Magnetization definition for different number of magnets.

These 2D simulations allow to define the size of the magnets according to the required lift force. The latter is defined by the mass of the vehicle and a 2D-3D ratio. It is represented on the left graph below by a dashed line.

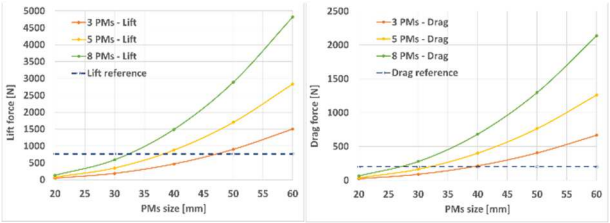

Fig. 6. Lift and Drag forces for different number of magnets.

The choice is made for five square magnets of 40x40x40 mm. This choice is justified by the size of the L-shape rail. For manufacturing reasons, the number of magnets is limited to five for the Halbach array. To assemble a Halbach array by hand (max force between magnet 110 N) the maximal size of the square PMs is 15 mm. Bigger PMs are mounted with mechanical assistance and a crimped system is necessary. The maximum force for the selected Halbach array is estimated at 908 N. Assembling more than five magnets is not recommended by the manufacturer. As there is no levitation at zero speed and while the drag force is high at low speed, the vehicle is equipped with wheels. These wheels raise the Halbach arrays by 5 mm to reduce the drag force at low speed and so to produce higher resulting propulsion force to launch the vehicle. The levitation force required for one Halbach array is about 345 N. The flight heights corresponding to this lift force for different speeds were plotted in blue in Fig. 7.

In red the equivalent drag forces in relation to speed is presented.

D. Damping

The size of the magnet chosen requires a crimp as explained in the previous chapter. Several alternatives were studied, including the use of an aluminium box. It has two utilities: to secure/keep the Halbach arrangement and to reduce the oscillation of the vehicle especially during the take-off. The damping effect has been demonstrated with FEA simulations. The simulated model is shown in Fig. 8.

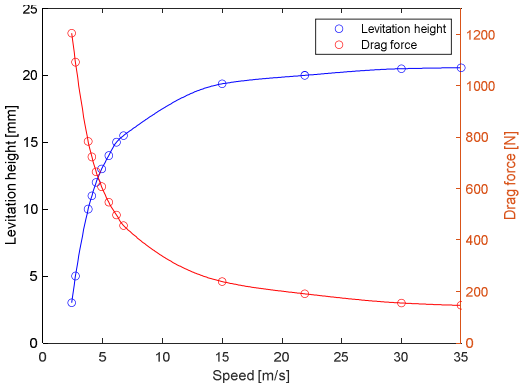

Fig. 7. Levitation height (blue) and drag force (red) in relation to the speed for a L-configuration with a 5PM Halbach array.

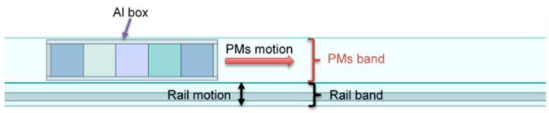

Fig. 8. Band and motions setup in the FEA environement ANSYS Maxwell

The software imposes only one direction of movement into a band of motion. For this reason, two bands are needed, one for X-direction of the magnets (vehicle movement) and a second for the Y-direction of the rail (vehicle oscillation). The negative and positive movement limits are defined by the bands. Disturbance results shown in this paper are caused by moving the system out of its equilibrium position with a variation of +3mm. The Y-position and the lift force are compared in the graphs below between a system with an aluminium box (thickness of 5mm) and without.

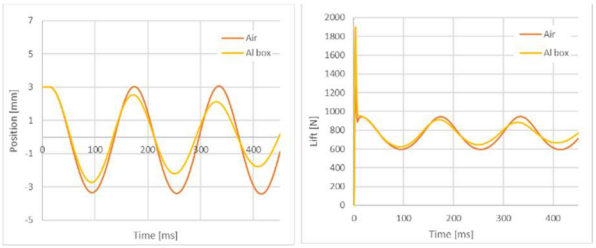

Fig. 9. Damping effect of the aluminum box on the position and lift

A damping coefficient of 89 Ns/m is observed for the system. The damping depends on the thickness of the aluminium box and the mass of the vehicle. A 7 mm box provides the best damping for our specifications. This damping is negligible compared to a mechanical damping, but still allows to decrease the oscillation peak in the launcher.

IV. DYNAMIC BEHAVIOR OF THE VEHICLE

A. Theroetical approach

To ensure that the vehicle remains in the guidance zone, the air gap variations are analysed throughout the run by simulating the dynamic behaviour of the vehicle. It is modelled as a set of point masses connected by ideal weightless spring and dampers. A system of differential equations for the motion of the nodes is given by applying Newton's second law to the nodes. The force is the sum of external forces (due to aerodynamic, launcher, magnetic, gravity, contacts, brakes) and the forces applied by the springs and dampers. The system is numerically integrated over time with the SciPy library considering the initial conditions (vehicle at standstill). It provides the dynamic behaviour in 6 degrees of freedom of the vehicle's centre of gravity and the evolution of the vertical and lateral air gaps of the Halbach arrays with the rails.

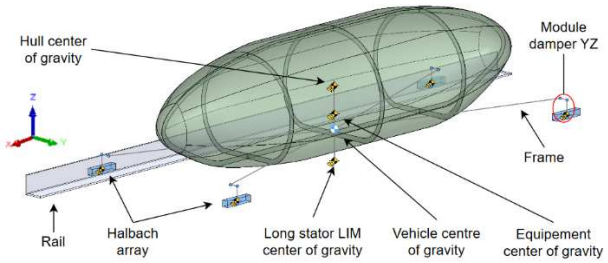

Fig. 10. Vehicle modelled as a set of point masses

The YZ dampers used to connect the levitation modules to the chassis are of the viscoelastic type and the simulation conditions for the L-rails are as follows (the conditions are similar for the V-rails but with different suspensions depending on the rail angle):

- Continuous launcher thrust: 8000N
- Length of launcher: 10m
- Rail oscillations Y & Z : 4mm every 20m

$$\delta_{rail}(x) = 0.004/2 * \sin(x * 2\pi/20) \quad (1)$$

- Vehicle travel distance: 97m
- Levitation damping coefficient: $c_{lev} = 89\ Ns/m$
- Verticals dampers: $k_z = 86300N/m;\ \xi_z = 0.584$
- Lateral dampers: $k_y \quad 2600N/m;\ \xi_y \quad 0.25$
- Deceleration: 8g
- Y-distance of wheel contact: 10mm
- Z-distance of wheel contact: 5mm

The magnetic force equations used in the simulation are fitted to the results obtained in section III and the lateral guidance force is defined as 10% of the levitation force. Their variables are the velocity v_{lev} of the module in the rail direction, the velocity v_{nlev} normal to the rail and the air gap δ_{lev} of the Halbach arrays.

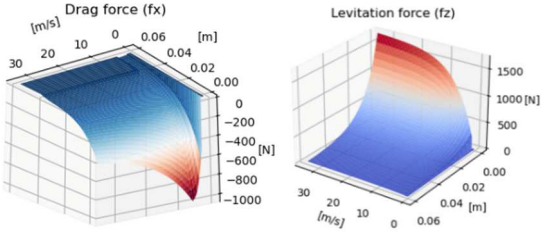

Fig. 11. Profile of the magnetic forces used for $\overrightarrow{v_{nlev}} = \vec{0}$

Forces are defined as follows:

Magnetic

$$\begin{aligned} F_{mag} &= f_{lift}\left(\overrightarrow{v_{lev}}, \overrightarrow{\delta_{lev}}\right)\overrightarrow{e_n} \\ &+ f_{lat}\left(\overrightarrow{v_{lev}}, \overrightarrow{\delta_{lev}}\right)\overrightarrow{e_{lat}} \\ &+ f_{drag}\left(\overrightarrow{v_{lev}}, \overrightarrow{\delta_{lev}}\right)\overrightarrow{e_x} - c_{lev}\,\overrightarrow{v_{nlev}} \end{aligned} \quad (2)$$

Damper Y&Z

$$\begin{aligned} \overrightarrow{F_{damp_l}} &= \left(-k_y\,\Delta y_l - 2\xi_y\sqrt{k_y\,m_{module}}\,\Delta\dot{y}_l\right)\overrightarrow{e_y} \\ &+ \left(-k_z\,\Delta z_l - 2\xi_z\sqrt{k_z\,m_{module}}\,\Delta\dot{z}_l\right)\overrightarrow{e_z} \end{aligned} \quad (3)$$

B. Results of simulation

During acceleration, the vehicle lifts up rapidly (Fig. 12),

which induces an oscillation that, if the magnets are attached directly to the frame, will be felt throughout the run due to the low damping of the EDS. Placing a damping device between the magnets and the frame reduces the amplitude and relaxation time of the transient regime (Fig. 13). This also avoids exciting a resonant frequency of the system by potential rail defects and thus ensures a constant airgap of the magnets in relation to the rails. Therefore, the mechanical suspension helps maintaining the EDS in its optimal air gap range (>20mm, see Fig. 13) despite dynamic perturbances and thus reduces the overall drag. Indeed, in these conditions, the levitation system has a quasi-linear magnetic drag which results in a linear speed reduction along the track (Fig. 15).

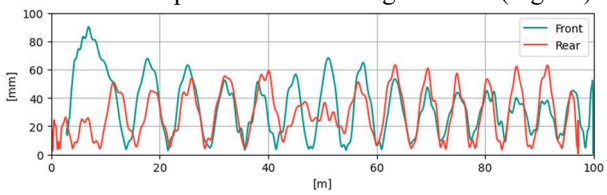

Fig. 12. Levitation airgaps according to X-position on L-rail without dampers and aluminium cage ($c_{lev} = 0$)

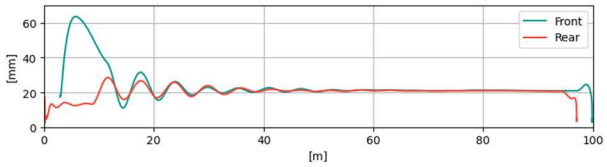

Fig. 13. Levitation airgaps according to X-position on L-rail with damper

For lateral guidance, as the magnetic forces considered are low, maintaining sufficient airgap to ensure guidance without the wheels touching the rail depends on fine-tuning the stiffness of the dampers. In these conditions, it is necessary to opt for soft dampers, but this allows the vehicle to yaw slightly, which is observed by an oscillation of the lateral airgaps (Fig. 14) without the vehicle's centre of mass moving sideways.

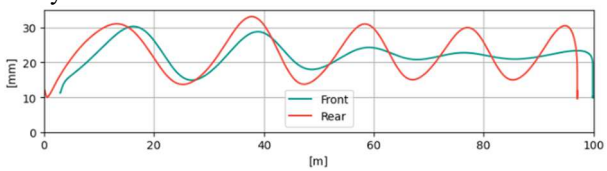

Fig. 14. Guide airgaps according to X-position on L-rails

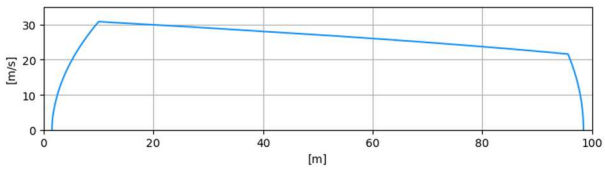

Fig. 15. Longitudinal speed of the vehicle's centre of gravity for L-rails

On V-rails, the greater the rail angle, the more unstable the vehicle is in roll. This is due to the low lateral drag of the Halbach arrays not exerting sufficient force to maintain the vehicle's Y-position and the lack of side guides to prevent the vehicle from running off the rails. Using flat V-rails can also be problematic when the shock absorbers are compressed inwards to the point where they can come off the rail and hit a sleeper. These effects are particularly noticeable at the 30° and 50° inclinations tested, but hardly at 10° (Fig. 16) without significant initial disturbance.

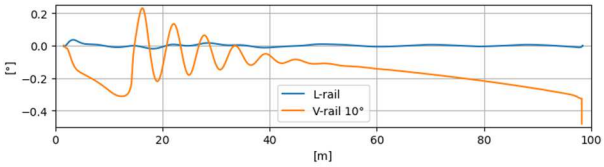

Fig. 16. Roll for rail types according to the position of the vehicle's centre of gravity

On L-rails, using soft, under-damped dampers ($0.25 < \xi_z < 1$) is a good compromise to ensure proper stability in all 6 degrees of freedom. Too much stiffness causes too much bounce and too high a damping ratio does not dissociate the magnets from the frame enough during acceleration, thus increasing the air gap too much.

V. Conclusion

To minimise air gap variations due to high acceleration, the use of optimised dampers is essential and mechanically constraining the guidance during the acceleration phase to reduce the initial pitch is a way to quickly achieve system stability.

Using a dynamic simulation model of the vehicle allows, beyond the evolution of the air gaps or the validation of the global concept, to understand the effect of rail defects, to predict its behaviour in non-standard conditions (e.g. high acceleration) and above all to dimension safety systems such as the brakes or the guides.

This article presents electromagnetic and damping characteristics of an EDS studied by using 3D FEM method. These results integrated in a quasi-static metamodel allow to analyse the drag and levitation forces on the system's dynamic. The design of the Halbach array to achieve the required dynamic performances for 2 guidance/levitation configurations and their advantages were presented. The obtained results show that it is possible to use only one Halbach array for the guidance and the levitation. The test of the vehicle (planned in the beginning of 2024) will allow to have a better knowledge of the dynamic behaviour at high speed in vacuum tube.

Acknowledgment

The authors gratefully acknowledge the collaboration with the Eurotube foundation. Thank you to Prof. Christophe Besson and Andres Gil Cladera from the IESE institute at the HEIG-VD who provided research support for the EDS design. The authors also would like to thank the HES-SO for their support of the GRIPIT project.

REFERENCES

[1] G. Pareschi et al., «Potential Analysis for vacuum Transport Technologies in the Public Transport Infrastructure of Switzerland, Technical Summary,» *Federal Office of Transport FOT, Bern, Switzerland,* 2023.

[2] P. Wang, L. Shi et R. zhang, «Design Optimization on Secondary and Performance Improvement of Long Primary Double-Sided Linear Induction Motor,» chez *22nd International Conference on Electrical Machines and Systems (ICEMS)*, 2019.

[3] K. Baoquan, Z. He et Y. Xiangrui, «Research on Long Stroke Moving Secondary Permanent Magnet Linear Eddy Current Brake,» *Transactions on Electrical Machines and Systems, 2019.*

[4] M. Flankl, T. Wellerdieck, A. Tüysüz et J. W. Kolar, «Scaling laws for electrodynamic suspension in high-speedtransportation,» *IET Electric Power Applications,* vol. 12, n° %13, pp. 357-364, 2018.

[5] S. S. e. al., «Dynamic Modeling and Simulation of Propulsion and Levitation Systems for Hyperloop,» chez *International Symposium on Linear Drives for Industry Applications*, Wuhan, China, 2021.

[6] M. Z. e. al., «Analysis of Electromagnetic and Damping Characteristics of Permanent Magnet Electrodynamic Suspension System,» chez *International Symposium on Linear Drives for Industry Applications*, Wuhan, China, 2021.